Large deviations of the average shapes of vesicles from equilibrium: Effects of thermal fluctuations in the presence of constraints

Volkmar Heinrich,[1,*] France Sevšek,[1,2] Saša Svetina,[1,2] and Boštjan Žekš[1,2]
[1]*Institute of Biophysics, Medical Faculty, Lipičeva 2, University of Ljubljana, SI-1000 Ljubljana, Slovenia*
[2]*J. Stefan Institute, Jamova 39, University of Ljubljana, SI-1000 Ljubljana, Slovenia*
(Received 3 September 1996)

In the absence of external stresses, the surface area and the volume of a closed, flaccid lipid vesicle are practically constant. Thermal shape fluctuations of vesicles that are subject to these constraints recently have been shown to induce a shift of the average shapes away from the equilibrium (zero temperature) shapes. Since only the average shapes can be determined from observations by optical microscopy, it is important to establish the magnitude of their deviation from the well-studied equilibrium shapes. In this paper we develop a formalism to calculate this thermal shift, and we demonstrate that nonlinearities in the constraints may cause it to be unexpectedly large. Allowing for arbitrary shape deformations, we present numerical calculations revealing a logarithmic dependence of the thermal shift on the number of fluctuational degrees of freedom of the vesicle membrane or, equivalently, on the number of lipid molecules constituting the membrane. As a consequence, the surface area (''projected area'') and, to a lesser extent, the volume (''projected volume'') of the average shape are smaller than their true values. These numerical results are in general agreement with theoretical predictions that have been made so far only for pieces of flat membranes but not for closed lipid membranes subject to the constraints of both constant area and volume. Furthermore, we derive an expression for the correlation function of deviations from equilibrium including terms of the order of $(k_BT)^2$ that involve the (quadratic) thermal shift. We demonstrate that these terms may actually exceed the commonly used leading term of the correlation function. This analysis suggests that the determination of the membrane bending modulus k_c from observations of thermal vesicle shape fluctuations should be based on the variances rather than the correlation functions. [S1063-651X(97)05902-3]

PACS number(s): 87.10.+e, 05.40.+j, 68.10.−m

I. INTRODUCTION

Flaccid phospholipid vesicles with volume-to-area ratios smaller than that of a sphere are known to exhibit thermal shape fluctuations that can be observed in an optical microscope [1]. While the different shapes of a fluctuating vesicle are governed by the elastic bending energy of the vesicle membrane, both its membrane area, as well as the volume of the enclosed aqueous solution, remain practically constant during observation. Such a vesicle is a typical example for a thermally excitable system that is subject to constraints [1,2]. Vesicle shape fluctuations have been intensively studied experimentally, mainly to deduce the value of the membrane bending modulus k_c [3]. The models used to interpret the experimental observations were usually based on a second-order expansion in terms of the deviations of the vesicle shape from a sphere, thus restricting the analysis to nearly spherical vesicles. Mathematical methods of much greater generality have been applied to study the equilibrium shapes of vesicles [4,5]. The results have been arranged in a ''phase diagram'' of equilibrium shapes that is in reasonable agreement with experimental observations [6,7,5]. On the other hand, general theoretical studies of the effect of thermal fluctuations on the vesicle shape have long been missing. The complications that arise from the presence of constraints only recently have been tackled theoretically in various, more systematic ways [8,2]. It was predicted that in the presence of constraints, a vesicle's thermal average shape may deviate from the equilibrium shape (''thermal shift'') [2]. Expanding the vesicle shape in a series of independent basis functions, the thermal shift may be represented by the average deviations of the amplitudes of basis functions from their equilibrium values. The lowest-order nonvanishing contribution to this shift has been shown to be proportional to k_BT. Since the leading term for a ''typical fluctuation'' (square root of the amplitude-amplitude correlation function of deviations from equilibrium) is of the order of $\sqrt{k_BT}$, it was argued [2] that the thermal shift should be small. On the contrary, we present numerical results revealing large values of the linear shift in the symmetry-conserving fluctuation modes. Moreover, we demonstrate that the shift diverges logarithmically as the number of fluctuation modes included in the calculations is increased.

To understand this effect of short-wavelength fluctuations, it is useful to recall first that for typical values of the membrane bending modulus $[k_c \approx (10-40)k_BT]$ the persistence length [9] of a phospholipid membrane is much larger than the characteristic vesicle size. It is justified, therefore, to treat the bilayer membranes considered here as ''almost planar'' surfaces in the sense that they maintain a certain regular mean shape. Nevertheless, on a microscopic scale a vesicle membrane represents a highly dynamic system that exhibits, due to its small resistance to bending, permanent thermal undulations about the mean shape. Most of these undulations

*FAX: (+386 61) 131-51-27. Electronic address: volkmar@sizif.mf.uni-lj.si

are too fast and too small in amplitude to be resolved in a light microscope. Yet one has to be aware that an image of an apparently smooth vesicle membrane comprises a large number of superimposed ''microstates'' where each state is characterized by a differently curved membrane. Although the curvatures involved may be small, the contributions of the large number of independent fluctuation modes sum up to result in a considerable vesicle-size-dependent reduction of the visible, apparent membrane area. This entropic effect has been noted quite some time ago, and it has been studied in detail for flat pieces of nonstretchable membrane [10–13] but not yet for closed membranes including simultaneously both constraints of membrane area and vesicle volume. Considering an isolated membrane piece, it was shown that the amount of membrane area that is taken up by mostly invisible, short-wavelength undulations depends logarithmically on the number of fluctuation modes [10–13]. As a consequence, a logarithmic correction of the bending modulus was predicted [11–13]. Incorporating the decrease of effective area into force balance equations via an ''entropic tension,'' the bending modulus of lipid membranes could be deduced from low-pressure aspiration of vesicles into micropipettes [14].

In these studies, the effective reduced area was taken to be the mean area of the ''projection'' of the fluctuating membrane piece onto a plane, resulting in the notion of the ''projected area.'' Naturally, this plane projection is also the *average shape* of the membrane piece. Analogously, we identify a vesicle's projected area with the area of its thermal average shape, while the volume of the average shape is taken to be the ''projected vesicle volume.'' In this paper, we set up a numerical formalism to obtain the average vesicle shape by calculating the expectation values of the amplitudes of the chosen set of basis functions describing the vesicle shape. This is done in two steps. First, the equilibrium shape is obtained by minimizing the membrane bending energy at constant values of membrane area and vesicle volume. Second, the linear averages of those deviations from the equilibrium shape that conserve both constraints are calculated. Both parts of the calculation are carried out using consistently the same set of basis functions. This calculation gives us, at the same time, the values of the projected membrane area and the projected vesicle volume as well as their logarithmic dependence on the number of fluctuation modes.

As another important consequence of the large thermal shift, we reconsider the calculation of the correlation function [15] of a fluctuating vesicle. The shift may be expected to enter this function in terms that are of higher order than the commonly used leading term proportional to k_BT. We outline a procedure to calculate the $(k_BT)^2$ contributions to the correlation function that contain the shift quadratically, and we show that they may indeed exceed the leading term. This procedure enables us to evaluate correctly the visible shape fluctuations represented by the mean-square deviations from the mean shape (variances).

The paper is organized as follows. In Sec. II we outline the theoretical basis for our treatment of constrained fluctuations in general terms and we derive the expressions to calculate the thermal shift as well as the correlation function. The application of this formalism to the numerical computation of the thermal average shape of a fluctuating vesicle is explained in Sec. III. Section IV presents the numerical results and discusses implications for related experiments. It is followed by a short conclusion given in Sec. V.

II. CONSTRAINED FLUCTUATIONS

The problem of constrained fluctuations is not specific to vesicle shapes; therefore, we will explain our treatment in general terms in the following. We start from an energy potential $W=W(x_1,\ldots,x_n)$ and α constraints ($\alpha<n$) given by $D_j(x_1,\ldots,x_n)=0$ ($j=1,\ldots,\alpha$). In the case of vesicle shape fluctuations, the variables $(x_1,\ldots,x_n)$ will be the amplitudes of independent, orthonormal basis functions. For a physical system in general, we identify them with Cartesian coordinates in an n-dimensional Euclidean phase space with basis vectors $\mathbf{i}_i$ ($i=1,\ldots,n$).

The states within this phase space that simultaneously satisfy all α constraints form the $(n-\alpha)$-dimensional subspace of *accessible* states, meaning that the system is bound to move exclusively within this subspace. Considering only the energies associated with points in this subspace, an equilibrium state is characterized by a minimum of the energy W with respect to any other *accessible* state in the vicinity of this point. We assume that the subspace of accessible states is ''well behaved'' near equilibrium, i.e. (in the language of differential geometry), that it is an $(n-\alpha)$-dimensional Riemannian manifold $M^{n-\alpha}$ that is continuous and differentiable at least to order 3 (a ''hypersurface'' embedded in the n-dimensional phase space). This hypersurface is represented in parameter form by

$$\mathbf{S}(q_1,\ldots,q_{n-\alpha})=x_1(q_1,\ldots,q_{n-\alpha})\mathbf{i}_1+\cdots+x_n(q_1,\ldots,q_{n-\alpha})\mathbf{i}_n, \tag{1}$$

where the q_k ($k=1,\ldots,n-\alpha$) are affine curvilinear coordinates adopted to this surface. The origin of the new reference frame is chosen at the equilibrium point (denoted below by the index 0), so that the equilibrium state is represented by $\mathbf{S}(0,\ldots,0)$.

For the treatment of thermal fluctuations we need to consider only small deviations from equilibrium. Thus we may replace the functions $x_i(q_1,\ldots,q_{n-\alpha})$ [$i=1,\ldots,n$; Eq. (1)] by their expansions around the equilibrium point. For reasons that will become evident below, this expansion is made up to the third-order terms in q_k, i.e.,

$$\Delta x_i(q_1,\ldots,q_{n-\alpha})=\sum_{k}^{n-\alpha} a_k^i q_k+\tfrac{1}{2}\sum_{k_1}^{n-\alpha}\sum_{k_2}^{n-\alpha} b^i_{k_1k_2}q_{k_1}q_{k_2}+\tfrac{1}{6}\sum_{k_1}^{n-\alpha}\sum_{k_2}^{n-\alpha}\sum_{k_3}^{n-\alpha} c^i_{k_1k_2k_3}q_{k_1}q_{k_2}q_{k_3}, \tag{2}$$

with the expansion coefficients $a^i_k\equiv(\partial x_i/\partial q_k)|_0$, $b^i_{k_1k_2}\equiv(\partial^2 x_i/\partial q_{k_1}\partial q_{k_2})|_0$, and $c^i_{k_1k_2k_3}\equiv(\partial^3 x_i/\partial q_{k_1}\partial q_{k_2}\partial q_{k_3})|_0$. (Here and in the following we denote by Δ the deviations from equilibrium. Furthermore, throughout the paper the starting index of all sums is 1 and is omitted.) Based on Eq. (2), we are able to express both the thermal shift $\langle\Delta x_i\rangle$ as

well as the correlation function $\langle \Delta x_{i_1} \Delta x_{i_2} \rangle$ in terms of expectation values involving only the new coordinates q_k.

So far, the expansion coefficients a^i_k, $b^i_{k_1 k_2}$, and $c^i_{k_1 k_2 k_3}$ define curvilinear coordinates q_k spanning an arbitrary $(n-\alpha)$-dimensional surface containing the equilibrium point. By imposing appropriate conditions on these expansion coefficients, we will, in the following, (i) ensure that the states forming this surface fulfill the constraints, (ii) choose suitable directions for (the tangents to) the coordinates q_k at equilibrium, and (iii) ensure that the coordinates q_k are orthonormal. The first requirement is fulfilled (up to third order at equilibrium) if the first, second, and third derivatives of all constraints $\widetilde{D}_j$ with respect to the q_k vanish at equilibrium. (The tilde is used to denote the functional dependence on q_k.) Thus

$$\left.\frac{\partial \widetilde{D}_j}{\partial q_k}\right|_0 = \sum_i^n \left.\frac{\partial D_j}{\partial x_i}\right|_0 a^i_k = 0, \tag{3a}$$

$$\left.\frac{\partial^2 \widetilde{D}_j}{\partial q_{k_1} \partial q_{k_2}}\right|_0 = \sum_{i_1}^n \sum_{i_2}^n \left.\frac{\partial^2 D_j}{\partial x_{i_1} \partial x_{i_2}}\right|_0 a^{i_1}_{k_1} a^{i_2}_{k_2} + \sum_i^n \left.\frac{\partial D_j}{\partial x_i}\right|_0 b^i_{k_1 k_2} = 0, \tag{3b}$$

and

$$\begin{aligned}\left.\frac{\partial^3 \widetilde{D}_j}{\partial q_{k_1} \partial q_{k_2} \partial q_{k_3}}\right|_0 = & \sum_{i_1}^n \sum_{i_2}^n \sum_{i_3}^n \left.\frac{\partial^3 D_j}{\partial x_{i_1} \partial x_{i_2} \partial x_{i_3}}\right|_0 a^{i_1}_{k_1} a^{i_2}_{k_2} a^{i_3}_{k_3} \\ & + \sum_i^n \left.\frac{\partial D_j}{\partial x_i}\right|_0 c^i_{k_1 k_2 k_3} + \sum_{i_1}^n \sum_{i_2}^n \left.\frac{\partial^2 D_j}{\partial x_{i_1} \partial x_{i_2}}\right|_0 \\ & \times (a^{i_1}_{k_1} b^{i_2}_{k_2 k_3} + a^{i_1}_{k_2} b^{i_2}_{k_1 k_3} + a^{i_1}_{k_3} b^{i_2}_{k_1 k_2}) = 0,\end{aligned} \tag{3c}$$

where $j = 1, \ldots, \alpha$ and $k, k_{1,2,3} = 1, \ldots, n-\alpha$.

Through the functions $\Delta x_i(q_1, \ldots, q_{n-\alpha})$ [Eq. (2)] the thermal energy of accessible states may be expressed as a function of new coordinates $\Delta \widetilde{W} = \Delta \widetilde{W}(q_1, \ldots, q_{n-\alpha})$. Assuming that *this* energy potential (i.e., *of accessible states*) has a harmonic shape near equilibrium, we neglect all higher-than-second-order terms in the energy expansion around equilibrium. For arbitrarily chosen coordinates q_k, the matrix of second derivatives of the energy with respect to those deviations that conserve the constraints (i.e., with respect to the q_k) is then diagonalized. Suppose we have chosen the coordinates q_k in such a way that this matrix is already diagonal [by requiring that the tangent vectors at equilibrium, $(\partial \mathbf{S}/\partial q_k)|_0$, have the same directions as the eigenvectors of this matrix]. Then, $(\partial^2 \widetilde{W}/\partial q_j \partial q_k)|_0 = \delta_{jk} \gamma_k$, where the γ_k denote the eigenvalues, and

$$\Delta \widetilde{W}(q_1, \ldots, q_{n-\alpha}) = \tfrac{1}{2} \sum_k^{n-\alpha} \gamma_k q_k^2. \tag{4}$$

The calculation of the eigenvalues γ_k is consistent with a second-order expansion of the constraints. Thus it would require one to include only the terms up to second order in q_k in the expansion (2). However, in the following we will include all those terms [up to the order of $(k_B T)^2$] in the calculation of the correlation function that originate from up to fourth-order deviations in the space of q_k, which makes it necessary to include also the third-order terms in the expansion (2).

Assuming that the states allowed by the constraints are *homogeneously distributed* within the hypersurface of accessible states, the average of an arbitrary function $f(x_1, \ldots, x_n)$ over all accessible states is given by

$$\langle f \rangle = \frac{\int_{M^{n-\alpha}} \widetilde{f} \exp(-\beta \Delta \widetilde{W}) dq}{\int_{M^{n-\alpha}} \exp(-\beta \Delta \widetilde{W}) dq}. \tag{5}$$

[The probability of an accessible state has been assumed to be given by the Boltzmann distribution, i.e., $\beta \equiv 1/k_B T$, and $dq \equiv dq_1 dq_2 \cdots dq_{n-\alpha}$.] Note that Eq. (5) is only correct if the volume element in the q space does not depend on the position within this space. This is achieved by requiring that the coordinates q_k form an orthonormal coordinate system at every point of the q space or, in other words, that the tangent vectors $\partial \mathbf{S}/\partial q_k$ be everywhere orthonormal. It would be cumbersome to enforce this condition strictly; instead, we will require orthonormality ''up to third order'' at equilibrium. Thus we require $(\partial \mathbf{S}/\partial q_k \cdot \partial \mathbf{S}/\partial q_j)|_0 = \delta_{jk}$ (the orthogonality part of this condition is already contained in the requirement that the directions of tangent vectors at equilibrium coincide with those of eigenvectors) and, furthermore, that the first and second derivatives of this orthonormality condition vanish at equilibrium. The resulting conditions for the expansion coefficients a^i_k, $b^i_{k_1 k_2}$, and $c^i_{k_1 k_2 k_3}$ read (where $k_{1,2,3,4} = 1, \ldots, n-\alpha$)

$$\sum_i^n a^i_{k_1} a^i_{k_2} = \delta_{k_1 k_2}, \tag{6a}$$

$$\sum_i^n a^i_{k_1} b^i_{k_2 k_3} = 0, \tag{6b}$$

$$\sum_i^n (b^i_{k_1 k_2} b^i_{k_3 k_4} + a^i_{k_1} c^i_{k_2 k_3 k_4}) = 0. \tag{6c}$$

Eventually, by combining the conditions (3a)–(3c) and (6a)–(6c) with our choice for the directions of tangent vectors at equilibrium, the system of curvilinear coordinates q_k has been completely defined.

Identifying $\widetilde{f}$ in Eq. (5) with Δx_i, replacing Δx_i by the expansion (2), inserting Eq. (4), and evaluating the resulting integrals up to the second order in q, the thermal shift in the original Cartesian coordinates is obtained up to terms of the order of $k_B T$ as

$$\langle \Delta x_i \rangle = \frac{k_B T}{2} \sum_k^{n-\alpha} \frac{b^i_{kk}}{\gamma_k}. \tag{7}$$

In the same way, but including also the $(k_B T)^2$ terms generated by fourth-order q terms, the correlation function is found to be

$$\langle \Delta x_{i_1} \Delta x_{i_2} \rangle = k_B T \sum_{k}^{n-\alpha} \frac{a_k^{i_1} a_k^{i_2}}{\gamma_k} + \frac{(k_B T)^2}{2} \sum_{k_1}^{n-\alpha} \sum_{k_2}^{n-\alpha} \frac{a_{k_1}^{i_1} c_{k_1 k_2 k_2}^{i_2} + a_{k_1}^{i_2} c_{k_1 k_2 k_2}^{i_1} + b_{k_1 k_2}^{i_1} b_{k_1 k_2}^{i_2} + \frac{1}{2} b_{k_1 k_1}^{i_1} b_{k_2 k_2}^{i_2}}{\gamma_{k_1} \gamma_{k_2}}$$

$$= k_B T \sum_{k}^{n-\alpha} \frac{a_k^{i_1} a_k^{i_2}}{\gamma_k} + \langle \Delta x_{i_1} \rangle \langle \Delta x_{i_2} \rangle + \frac{(k_B T)^2}{2} \sum_{k_1}^{n-\alpha} \sum_{k_2}^{n-\alpha} \frac{a_{k_1}^{i_1} c_{k_1 k_2 k_2}^{i_2} + a_{k_1}^{i_2} c_{k_1 k_2 k_2}^{i_1} + b_{k_1 k_2}^{i_1} b_{k_1 k_2}^{i_2}}{\gamma_{k_1} \gamma_{k_2}}. \tag{8}$$

These results illustrate how nonlinearities in the constraints may qualitatively affect the behavior of the system. The first-order coefficients a_k^i, which are determined by the linearized constraints, define the $(n-\alpha)$-dimensional tangent ''plane'' to the hypersurface of accessible states at equilibrium, i.e., the tangent space that is spanned by the eigenvectors of the matrix of second derivatives of the energy with respect to deviations that conserve the constraints. This tangent space represents a first-order approximation to the hypersurface of accessible states and it is related to any $(n-\alpha)$-dimensional subspace spanned by a subset of original Cartesian coordinates x_i by a mere linear transformation. On the other hand, whenever the constraints are nonlinear, the hypersurface of accessible states is *curved*. In this case, projections of the accessible states (which were assumed to be homogeneously distributed within this hypersurface) onto the Cartesian coordinate axes x_i result in a *nonuniform density* of (projected accessible) states along these axes. This effect causes the energy potential to be asymmetric with respect to the x_i, which results in the nonvanishing thermal shift. It is important to note that this effect is purely geometrical, i.e., it depends only on the shape of the hypersurface of accessible states but not on the temperature. Mathematically, this effect is reflected by the higher-than-first-order coefficients in the nonlinear transformation Eq. (2).

The fact that the thermal shift is proportional to $k_B T$, whereas a ''typical fluctuation'' given by the leading term of $\langle \Delta x_{i_1} \Delta x_{i_2} \rangle^{1/2}$ is of the order of $(k_B T)^{1/2}$, has led to the conclusion [2] that the shift is small. However, given that the shift [Eq. (7)] and the leading term of the correlation function [Eq. (8)] depend on different, independent coefficients, it is important to establish also the magnitudes of these coefficients. In the case of vesicle shape fluctuations, we have found that for some values of i and k the coefficients b_{kk}^i may actually be two orders of magnitude larger than the a_k^i. In this case, the nonlinearities in the constraints generate quite large values of the thermal shift. These nonlinearities do not enter the leading term of the correlation function, yet one would expect that in this case, they also have a significant effect on this function. To establish the importance of this effect, we have included the $(k_B T)^2$ terms in the derivation of Eq. (8). The result shows that the thermal shift affects the correlation function directly in form of the products $\langle \Delta x_{i_1} \rangle \langle \Delta x_{i_2} \rangle$. These products may not be neglected if the shift is large. On the other hand, we will assume in the following that the nonlinearities of the constraints are represented to a good approximation by the second-order coefficients b_{kk}^i, and we will not attempt to include terms of even higher order (which would be practically impossible in the numerical calculations). For vesicle shape fluctuations, we have calculated for a few representative examples also the coefficients $b_{k_1 k_2}^i$ with $k_1 \neq k_2$, and we found them to be always significantly smaller than the values of the b_{kk}^i. For these reasons it seems to be justified to assume that the last $(k_B T)^2$ term on the right-hand side of Eq. (8) is small compared to the sum of the other two contributions, and so we will omit it in the following.

III. AVERAGE VESICLE SHAPE

Let us now apply this theoretical framework to the calculation of the average shape of a fluctuating vesicle. We consider vesicle shapes of *arbitrary symmetry*, with the *only restriction* that the shapes are single-valued functions of the spherical angles. Then, the shape can be described by the function $R = R(\vartheta, \varphi)$, where R points from the origin of the reference frame (suitably chosen inside the vesicle) to the vesicle surface. This shape function is expanded in the series

$$R(\vartheta, \varphi) = \sum_{i}^{(l_{\max}+1)^2} X_i p_i(\vartheta, \varphi), \tag{9}$$

where $p_i(\vartheta, \varphi)$ are the functions of the complete set $\{Y_{l0}, \mathrm{Re}(\sqrt{2} Y_{lm}), \mathrm{Im}(\sqrt{2} Y_{lm})\}$ of real, orthonormal basis functions derived from the spherical harmonics Y_{lm}, and $l_{\max}$ is the cutoff of the expansion if expressed in terms of the latter functions. The energy governing different vesicle shapes is the membrane bending energy [16,6]. It is the sum of a local and a nonlocal contribution [17] and, in general, both affect the shape fluctuations. However, in those regions in the phase diagram of equilibrium shapes where the nonlocal bending energy is zero or small, its effect on the shape fluctuations is very small as well and may be neglected. In this study we restrict our treatment to this region and do not include nonlocal bending effects. The remaining local bending energy reads for symmetric bilayer membranes

$$W = \tfrac{1}{2} k_c \int (C_1 + C_2)^2 dA, \tag{10}$$

where k_c is the (local) membrane bending modulus, $C_{1,2}$ are the principle curvatures, and integration is performed over the closed vesicle surface. Expressing this energy as well as the constraints of constant membrane area (put in the form $D_1 \equiv A - A_0 = 0$) and constant vesicle volume ($D_2 \equiv V - V_0 = 0$) in terms of the shape function $R(\vartheta, \varphi)$ [5], we arrive at the task to calculate fluctuations of a system with energy $W = W(X_1, \ldots, X_n)$ and with two constraints $D_{1,2}(X_1, \ldots, X_n) = 0$, which interrelate the $n = (l_{\max}+1)^2$ amplitudes X_i of the basis functions of the shape expansion [Eq. (9)]. As usual, we introduce dimensionless quantities by a

normalization with respect to a sphere (with radius R_S) having the same surface area as the vesicle. To distinguish normalized quantities from the respective original ones, we denote all normalized quantities by small letters. Thus, for example, the energy w is measured in units of $8\pi k_c$, while $r \equiv R/R_S$, $x_i \equiv X_i/R_S$, $c_i \equiv C_i R_S$, etc.

As the first step, we calculate the equilibrium shape at given membrane area and vesicle volume. For a given set of x_i, the values of model quantities (energy and constraints) and, as needed, of their first and second derivatives with respect to x_i are calculated numerically by a two-dimensional integration over the full solid angle. Using the generalized energy function

$$w^* = w + \sum_j^2 \lambda_j d_j \tag{11}$$

that includes the constraints via Lagrange multipliers λ_j, the equilibrium values of amplitudes x_i and of Lagrange multipliers are obtained by the Ritz method described in detail in [5].

To compute the thermal shift $\langle \Delta x_i \rangle$, we have to calculate the eigenvalues γ_k as well as the coefficients b^i_{kk} [Eq. (7)], whereas the third-order coefficients $c^i_{k_1 k_2 k_3}$ are not needed. In the practical calculations we first choose arbitrarily a solution out of the solution space of the (underdetermined) conditions (3a) and (6a). This solution space is most efficiently obtained by singular value decomposition of the $2 \times n$ matrix with elements $(\partial d_j/\partial x_i)|_0$. The chosen solution represents a preliminary set of first-order coefficients denoted by $\overline{a^i_k}$. Imposing condition (3b) on preliminary second-order coefficients $\overline{b^i_{k_1 k_2}}$, making use of the equilibrium condition, and introducing the generalized energy w^* [Eq. (11)], the second derivatives of the energy with respect to the (preliminary) affine coordinates $\overline{q_k}$ are found to be

$$w_{k_1 k_2} \equiv \left. \frac{\partial^2 \tilde{w}}{\partial \overline{q_{k_1}} \partial \overline{q_{k_2}}} \right|_0 = \sum_{i_1}^n \sum_{i_2}^n \left. \frac{\partial^2 w^*}{\partial x_{i_1} \partial x_{i_2}} \right|_0 \overline{a^{i_1}_{k_1}} \overline{a^{i_2}_{k_2}}.$$

Next, the matrix with elements $w_{k_1 k_2}$ is diagonalized, which gives the eigenvalues γ_k [Eqs. (4) and (7)], while the eigenvectors determine the directions of tangent vectors to the subspace of accessible states at equilibrium. Thus the final first-order coefficients are given by

$$a^i_k = \sum_j^{n-2} \overline{a^i_j} e_{jk},$$

where e_{jk} is the jth element of the kth eigenvector. The coefficients b^i_{kk} are then obtained from the systems of linear equations given by conditions (3b) and (6b). Finally, insertion of the results into Eq. (7) (where $k_B T$ is now divided by $8\pi k_c$) gives the thermal shift. It has been noted before [2] that contributions involving the zero eigenvalues corresponding to rigid-body motions have to be excluded from the sum in Eq. (7).

Then, the average vesicle shape is given by [cf. Eq. (9)]

$$\langle r(\vartheta,\varphi) \rangle = \sum_i^n (x_i|_0 + \langle \Delta x_i \rangle) p_i(\vartheta,\varphi), \tag{12}$$

where, as before, $n = (l_{\max}+1)^2$. The mean-square deviation of the shape function $r(\vartheta,\varphi)$ from its mean (variance) is

$$\begin{aligned} \langle (r - \langle r \rangle)^2 \rangle &= \langle r^2 \rangle - \langle r \rangle^2 \\ &= \sum_{i_1}^n \sum_{i_2}^n (\langle \Delta x_{i_1} \Delta x_{i_2} \rangle \\ &\quad - \langle \Delta x_{i_1} \rangle \langle \Delta x_{i_2} \rangle) p_{i_1}(\vartheta,\varphi) p_{i_2}(\vartheta,\varphi). \end{aligned}$$

Using Eq. (8) and neglecting the last term on its right-hand side, we find

$$\langle (r - \langle r \rangle)^2 \rangle = \frac{k_B T}{8\pi k_c} \sum_{i_1}^n \sum_{i_2}^n p_{i_1}(\vartheta,\varphi) p_{i_2}(\vartheta,\varphi) \sum_k^{n-2} \frac{a^{i_1}_k a^{i_2}_k}{\gamma_k}. \tag{13}$$

The square root of this expression gives the standard deviation of the shape function as a function of the spherical angles; it is a measure for the mean width of fluctuations at each point of the vesicle membrane.

Following Ref. [10], we call the area of the average shape ''projected area'' $\langle A_p \rangle$, while the volume of the average shape is called ''projected volume'' and is denoted by $\langle V_p \rangle$. The normalized deviations of these two quantities from their equilibrium values are given up to the order of $k_B T$ by

$$\langle \Delta a_p \rangle = \sum_i^n \left. \frac{\partial d_1}{\partial x_i} \right|_0 \langle \Delta x_i \rangle, \quad \langle \Delta v_p \rangle = \sum_i^n \left. \frac{\partial d_2}{\partial x_i} \right|_0 \langle \Delta x_i \rangle. \tag{14}$$

Here $\langle v_p \rangle = \langle V_p \rangle / \frac{4}{3}\pi R_S^3$, whereas the apparent relative volume is defined with respect to a sphere whose surface area is the apparent projected area $\langle A_p \rangle$. Denoting by $\hat{R}_S$ the radius of this sphere, this apparent relative volume is

$$\begin{aligned} \langle \hat{v}_p \rangle &= \frac{\langle V_p \rangle}{\frac{4}{3}\pi \hat{R}_S^3} = (v_0 + \langle \Delta v_p \rangle) \left(\frac{R_S}{\hat{R}_S} \right)^3 \\ &= \frac{v_0 + \langle \Delta v_p \rangle}{(1 + \langle \Delta a_p \rangle)^{3/2}} \cong v_0 + \langle \Delta v_p \rangle - \tfrac{3}{2} v_0 \langle \Delta a_p \rangle. \end{aligned} \tag{15}$$

IV. NUMERICAL RESULTS AND DISCUSSION

Our numerical calculations concentrate on the shape fluctuations of vesicles with relative volumes v_0 ranging from 0.8 to 0.95. The equilibrium shapes of these vesicles are axisymmetric with an additional reflection plane containing the equator. The membrane bending modulus is taken to be $k_c = 10^{-19}$ J, a typical value for phospholipid bilayers [18]. The temperature is chosen to be $T = 293$ K. In the numerical computations, the largest possible value of the cutoff $l_{\max}$ of the expansion of the shape function Eq. (9) is limited by the available computer memory. Presently, we are able to use $l_{\max}$ values up to 25.

Before turning to the calculation of the thermal shift it is useful first to rule out possible effects of an insufficient accuracy of the method due to too small values of $l_{\max}$. This

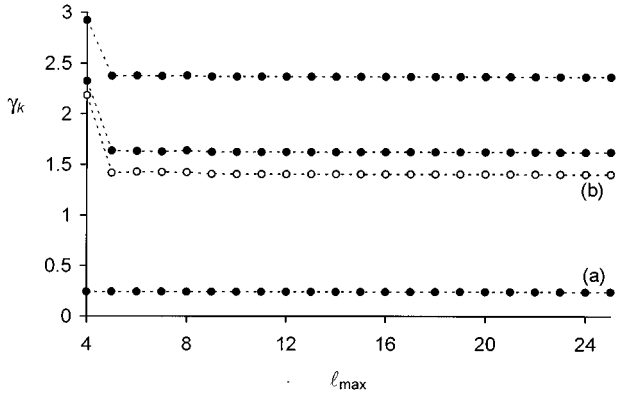

FIG. 1. Smallest nonzero eigenvalues γ_k of the matrix of second derivatives of the normalized bending energy with respect to deformations that conserve the constraints, as obtained at different values of the cutoff l_{max} of the shape expansion. Twofold degenerate eigenvalues are marked by filled circles. These values were calculated for an axisymmetric equilibrium shape with a relative volume $v_0=0.95$. Physically, the eigenmodes of an axisymmetric equilibrium shape group into sectors that are characterized by a given value of $|m|$ and either all possible even or all possible odd l's. If the eigenvalues are numbered in ascending order, the first five correspond to rigid-body motions and are zero (not shown). The pair of the smallest two nonzero eigenvalues [series (a)] corresponds to $|m|=2$, even-l deformations breaking the rotational symmetry in the direction of shapes with symmetry D_{2h}. The next eigenvalue [represented by open circles, series (b)] corresponds to the $m=0$, odd-l deformation breaking the up-down mirror symmetry and leading to pearlike shapes.

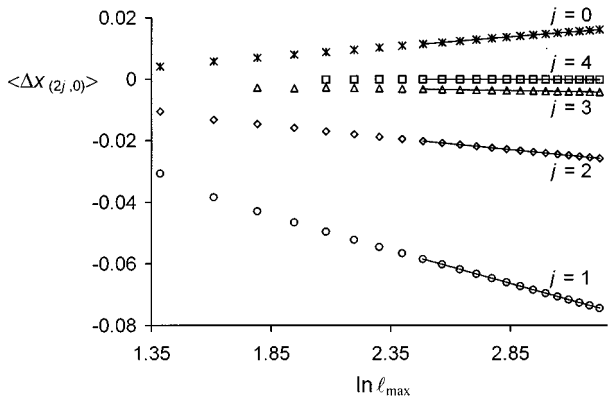

FIG. 2. Linear dependences of the thermal shifts $\langle \Delta x_{(2j,0)} \rangle$ (for $j=0,\ldots,4$) on the natural logarithm of l_{max}. The straight lines were obtained from linear fits to the numerically calculated ''data points'' in the l_{max} range from 12 to 25. The parameters are $v_0=0.95$, $k_c=10^{-19}$ J, and $T=293$ K.

can be done by inspecting the smaller eigenvalues γ_k [Eq. (4)], which should not depend on l_{max}. For axisymmetric shapes there are five zero eigenvalues corresponding to rigid-body motions. We have ''tuned'' the accuracy of our numerical computations such that at $v_0=0.95$, the calculated values of these five eigenvalues are for $l_{max} \geqslant 15$ all smaller than 10^{-7}. Another characteristic of axisymmetric shapes is that all eigenvalues corresponding to deformations breaking the rotational symmetry (i.e., $m \neq 0$ deformations) are twofold degenerate, which is due to the equivalence of deformations in the directions $\varphi=0$ and $\pi/2$, respectively. Figure 1 shows the smallest *nonzero* eigenvalues (i.e., those that dominate the near-equilibrium behavior of the fluctuating shape) calculated for $v_0=0.95$ as functions of l_{max}. It is seen that already at $l_{max}=6$ the ''true'' values of these eigenvalues are reproduced with a very high accuracy. By inspecting *all* $(l_{max}+1)^2-2$ eigenvalues as computed for different l_{max} values we found that most eigenvalues remain unaffected by an increase of l_{max}. Only those $4l_{max}$ eigenvalues that are the largest ones at a given l_{max} experience a noticeable correction when their values are computed at the next higher value of l_{max}. However, these eigenvalues are so large (their values being of the order of l_{max}^4) that they matter little for the fluctuations. It should be mentioned that at lower relative volumes, the eigenvalues ''stabilize'' only at higher values of l_{max}. For example, at $v_0=0.8$ any result obtained with $l_{max}<16$ will involve significant uncertainties caused by an inaccurate assessment of the true eigenvalues. This somewhat restricts also the applicability of the present method to vesicles with relative volumes $v_0 \geqslant 0.8$, although principally one could extend (at the cost of computer time and memory usage) the range of volumes down to $v_0 \approx 0.6$ by using higher values of l_{max}. Relative volumes smaller than $v_0 \approx 0.6$ cannot be considered because of the limitation of the present method to shapes that are single-valued functions of the spherical angles.

Using Eq. (7) we have calculated the thermal shifts at different values of l_{max}. For an equilibrium shape of given symmetry, linear net shifts occur only in the symmetry-conserving modes (cf. [2]) because all symmetry-breaking fluctuations ''average out.'' For the axisymmetric equilibrium shapes considered here, the symmetry-conserving modes are characterized by $m=0$ and even values of l. Identifying the indices i of amplitudes x_i of these modes with the corresponding pairs $(2j,0)$ of indices of spherical harmonics $Y_{2j,0}$, Fig. 2 shows for $j=0,\ldots,4$ the thermal shifts obtained at $v_0=0.95$ as functions of the natural logarithm of l_{max}. It is clearly seen that the thermal shift in these modes depends on l_{max}. This can be understood by taking into account that for nonlinear constraints, adding degrees of freedom by increasing l_{max} results in an uneven change of the density of projected (accessible) states along the Cartesian coordinate axes x_i. Since, in general, more states are added at a distance from equilibrium than in its close vicinity, the (absolute) thermal shift increases with l_{max}. By inspecting the values of the coefficients b^i_{kk} we found that *every* added degree of freedom affects, through the nonlinear constraints, the shifts in *all* symmetry-conserving modes. For the modes depicted in Fig. 2, the shift is already quite large at the highest l_{max} value used. It is worth comparing the squares of these thermal shifts $\langle \Delta x_{(2j,0)} \rangle^2$ with the lowest-order contributions to the mean squares $\langle \Delta x^2_{(2j,0)} \rangle$. The latter values are readily obtained from the first term on the right-hand side of Eq. (8). For $j=0,1,2$ the leading terms of the mean squares are found to be *smaller* than the respective values of $\langle \Delta x_{(2j,0)} \rangle^2$ at $l_{max}=25$ (for example, the leading term of $\langle \Delta x^2_{(2,0)} \rangle$ is as small as 2.54×10^{-5}, while $\langle \Delta x_{(2,0)} \rangle^2 \approx 0.005\,54$). Since the mean squares may not be smaller than the respective squares of the mean values, this means that omission of the large term proportional to $(k_BT)^2$ in Eq. (8) (being just the squared

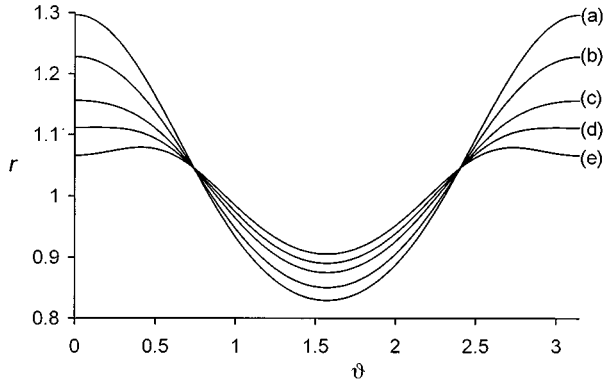

FIG. 3. Normalized shape functions $r(\vartheta,\varphi)$ of the equilibrium shape (a), of the average shape as calculated for $l_{\max}=25$ (b), and of the approximate average shapes estimated by extrapolation to $l_{\max}=10^3$ (c), $l_{\max}=10^4$ (d), and $l_{\max}=10^5$ (e). All shapes are axisymmetric; therefore, the shape functions are shown in dependence of ϑ. The parameters are the same as in Fig. 2.

shift itself) leads to meaningless values of the mean squares for these modes.

The results shown in Fig. 2, along with the analogous results obtained for the other modes and at different relative volumes, give us high confidence that the dependence of $\langle \Delta x_{(2j,0)} \rangle$ on $l_{\max}$ is logarithmic. Linear regressions to the numerically calculated dependences of $\langle \Delta x_{(2j,0)} \rangle$ on the natural logarithm of $l_{\max}$ (taking only the ''data points'' obtained for $l_{\max} \geqslant 12$) yielded practically ideal fits. The fitted straight lines are included in Fig. 2. Writing this dependence in the form

$$\langle \Delta x_i \rangle = \frac{k_B T}{8\pi k_c} (\mu_i \ln l_{\max} + \eta_i), \tag{16}$$

the coefficients μ_i, η_i can thus be determined with high accuracy from our results obtained for the relatively small range of $l_{\max}$ values that can be handled numerically. [For those values of i in Eq. (16) that correspond to symmetry-breaking deformations, of course, $\mu_i = \eta_i = 0$.] Assuming that this logarithmic dependence reflects the actual physical behavior correctly, we can readily estimate the (approximate) overall thermal shifts comprising the contributions of all degrees of freedom up to a realistic cutoff $l_{\max}$. The magnitude of such a cutoff may be obtained by identifying $l_{\max} = \sqrt{A_0 / A_{\mathrm{mol}}}$, where $A_0 = 4\pi R_S^2$ is the membrane area and A_{mol} is the typical area occupied by one (or a few) lipid molecule(s) in the vesicle membrane. For giant vesicles, i.e., vesicles whose fluctuations may be observed in a light microscope, R_S ranges from 5 to 50 μm, while $A_{\mathrm{mol}} \approx 0.6$–$0.7$ nm^2 is typical for a single lipid molecule. Thus $l_{\max} \approx 10^3$–10^5, where $l_{\max}$ increases linearly with the characteristic vesicle size R_S. For various values of $l_{\max}$, we have estimated the overall values of the thermal shifts in the low-l modes ($l \leqslant 16$) and calculated the corresponding approximate average shapes using Eq. (12). Figure 3 shows for $v_0 = 0.95$ the resulting shape functions together with that of the equilibrium shape. The large difference between the average shape obtained by extrapolation to the cutoff $l_{\max}=10^5$ and the equilibrium shape is illustrated in Fig. 4(a). The analogous result obtained at $v_0 = 0.8$ is shown in Fig. 4(b). Using Eq. (13) we have also calculated the standard deviations $\langle (r - \langle r \rangle)^2 \rangle^{1/2}$ at $l_{\max}=25$ (the variances show only a minor dependence on $l_{\max}$ and converge fast) for $v_0 = 0.95$ and 0.8. These standard deviations are included in the contour plots of the average shapes [Figs. 5(a) and 5(b)], where they denote the mean width of visible fluctuations about the mean shapes.

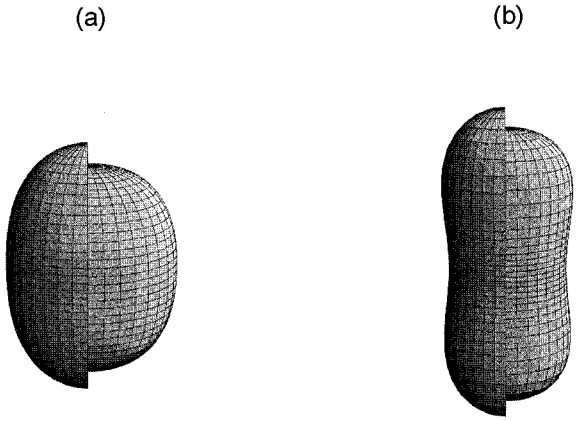

FIG. 4. (a) Comparison of the equilibrium shape (part on the left) with the approximate average shape (part on the right) obtained by extrapolation to $l_{\max}=10^5$ [$v_0 = 0.95$; cf. curve (e) in Fig. 3]. Both shapes were cut in half along the axis of rotation; one-half of each is shown. (b) Illustration of the analogous result obtained at $v_0 = 0.8$. The parameters are $k_c = 10^{-19}$ J and $T = 293$ K.

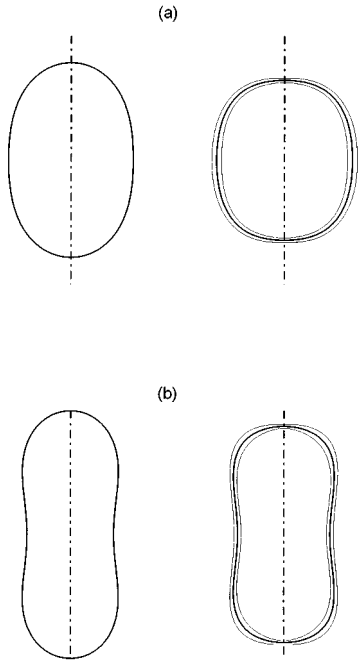

FIG. 5. Contour plots of the equilibrium shape (on the left) and of the average shape as obtained for $l_{\max}=10^5$ (on the right, thick line) at (a) $v_0 = 0.95$ and (b) $v_0 = 0.8$. The contour of the average shape is enclosed by thin lines denoting the mean width of visible fluctuations about this average shape. All shapes are axisymmetric; the vertical axis of rotation is included in each plot. The parameters are the same as in Fig. 4.

It is important to note that only the average shape, modulated by visible fluctuations, can be observed in an optical microscope. As illustrated in Figs. 4 and 5, this average shape may substantially deviate from the equilibrium shape. The thermal shift causes an apparently ''static'' deformation that may be significantly larger than the visible shape undulations and so it should be easily detectable in a light microscope. However, for this, one would need an accurate measure of the true values of the membrane area and the vesicle volume because these are basic control parameters determining the equilibrium shape. The only information about these parameters that has been used so far in the analysis of experimental observations was obtained from measurements of the visible vesicle contours. As mentioned above, such measurements can at most give the surface area and the volume of the average shape, i.e., the *projected* membrane area and the *projected* vesicle volume. Their deviations from the respective equilibrium values are given by Eqs. (14). Using Eq. (16), these deviations are rewritten as

$$\langle \Delta a_p \rangle = \frac{k_B T}{8\pi k_c} \sum_i^n \left. \frac{\partial d_1}{\partial x_i} \right|_0 (\mu_i \ln l_{\max} + \eta_i)$$

$$= \frac{k_B T}{8\pi k_c} (\mu^{(a)} \ln l_{\max} + \eta^{(a)}) \tag{17}$$

and analogously

$$\langle \Delta v_p \rangle = \frac{k_B T}{8\pi k_c} (\mu^{(v)} \ln l_{\max} + \eta^{(v)}), \tag{18}$$

where

$$\mu^{(a,v)} \equiv \sum_i^n \left. \frac{\partial d_{1,2}}{\partial x_i} \right|_0 \mu_i, \quad \eta^{(a,v)} \equiv \sum_i^n \left. \frac{\partial d_{1,2}}{\partial x_i} \right|_0 \eta_i. \tag{19}$$

Both the values of $(\partial d_j/\partial x_i)|_0$ $(j=1,2)$, as well as of the coefficients μ_i and η_i, converge fast towards zero as i is increased. Thus one may use relatively low values for the upper limit n in the sums in Eqs. (19) to obtain the coefficients $\mu^{(a)}$, $\eta^{(a)}$, $\mu^{(v)}$, and $\eta^{(v)}$ to a good approximation. At different relative volumes, we have estimated these sums by taking into account the first nine nonvanishing contributions. The coefficients $\mu^{(v)}$ of the logarithmic $l_{\max}$ dependence of the projected volume were found to be so small that significant effects of roundoff and truncation errors cannot be excluded. However, this small logarithmic contribution may safely be neglected even for large $l_{\max}$ values, so that the deviation of the projected volume from the equilibrium volume can be taken to be constant and proportional to $\eta^{(v)}$. All other coefficients show clear dependences on the relative vesicle volume that are depicted in Figs. 6(a) and 6(b). The dependence shown in Fig. 6(a) indicates that for closed vesicles, the logarithmic dependence of the area reduction cannot be described by a universal constant or by a universal constant *alone*. Yet the range of values is in very good agreement with the value $\mu^{(a)}_{\text{flat}} = -2$ obtained in [10,12,13] for flat membranes. The dependence of $\mu^{(a)}$ on the relative volume v_0 could also not be explained by the presence of a constant (but volume-dependent) surface tension because such a tension would show up only in the coefficient $\eta^{(a)}$ (cf. [10]). In our opinion, it is the combination of the two constraints, causing both a membrane tension *and* a pressure difference across the membrane (where both may fluctuate in order to conserve the constraints near equilibrium), that is responsible for the dependence shown in Fig. 6(a).

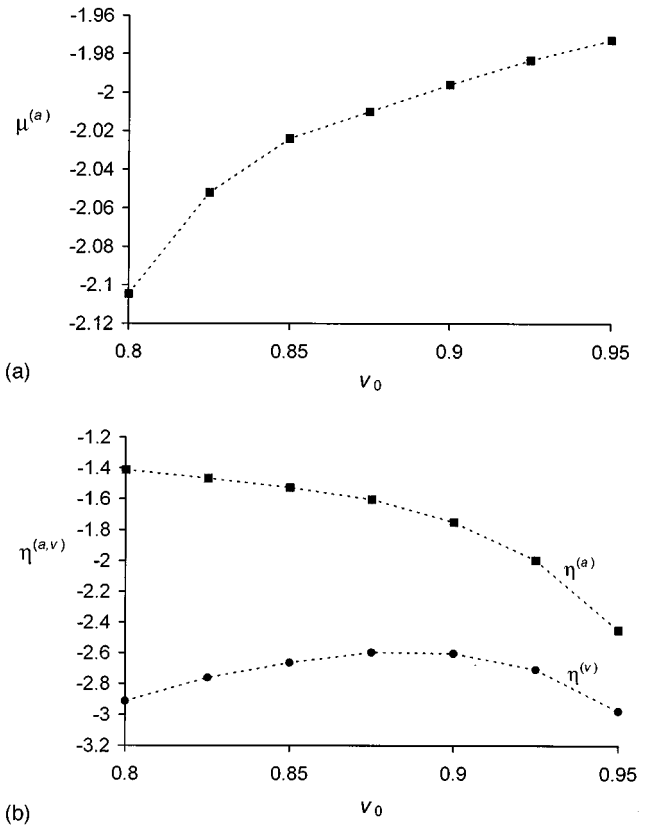

FIG. 6. (a) Coefficient $\mu^{(a)}$ of the logarithmic $l_{\max}$ dependence of the relative deviation $\langle \Delta a_p \rangle$ of the projected area from the true membrane area [cf. Eq. (17)] as a function of the relative vesicle volume v_0. (b) Analogous plot showing the dependences of the coefficients $\eta^{(a)}$ [Eq. (17)] and $\eta^{(v)}$ [Eq. (18)] on v_0. The parameters are the same as in Fig. 4.

For practical purposes, we may conclude from our numerical calculations that area and volume measurements based on the analysis of the visible vesicle contours will generally result in too small values of both the membrane area and the vesicle volume. While the reduction of the effective volume can be taken to be constant and relatively small, one has to be aware that area measurements may substantially underestimate the true membrane area, with an error that depends logarithmically on the vesicle size. In the interpretation of experimental observations, it is common to combine the results of these two measurements into a single control parameter. This is the (apparent) relative volume, i.e., the renormalized projected relative volume given by Eq. (15). With Eq. (16) it becomes

$$\langle \hat{v}_p \rangle = v_0 + \frac{k_B T}{8\pi k_c} \{ (\mu^{(v)} - \tfrac{3}{2} v_0 \mu^{(a)}) \ln l_{\max} + \eta^{(v)} - \tfrac{3}{2} v_0 \eta^{(a)} \}. \tag{20}$$

Table I gives estimates of $\langle \hat{v}_p \rangle$ for different relative volumes and $l_{\max}$ values. It is seen that the measured values of this

TABLE I. Estimates of the apparent relative volume $\langle \hat{v}_p \rangle$ [Eq. (20)] for different values of the true relative volume v_0 and at different values of $l_{\max}$. The range of $l_{\max}$ values corresponds roughly to characteristic vesicle sizes R_S ranging from 5 to 50 μm. The parameters are $k_c = 10^{-19}$ J and $T = 293$ K.

	$\langle \hat{v}_p \rangle$		
v_0	$l_{\max}=10^3$	$l_{\max}=10^4$	$l_{\max}=10^5$
0.8	0.825	0.835	0.844
0.85	0.877	0.887	0.896
0.9	0.929	0.939	0.949

important control parameter are likely to contain errors as large as 5% or even larger, depending on the value of the bending modulus k_c. Thus an independent measure of membrane area and vesicle volume could greatly increase the accuracy of experimental data obtained from the analysis of vesicle contours. Such a measurement is feasible by combining the contour analysis with a subsequent micropipette aspiration of the observed vesicle. The latter technique gives quite accurate values for membrane area and vesicle volume (cf., e.g., [19,18]). In addition, since the area-expansivity modulus of vesicle membranes can readily be established by micropipette aspiration, such a measurement could help to decide whether or not the observed vesicle is unilamellar.

Similar arguments apply to measurements of the membrane bending modulus k_c that are based on the analysis of thermal vesicle shape fluctuations. A logarithmic correction of k_c caused by invisible, short-wavelength undulations of flat membranes frequently has been discussed in the literature (e.g., [11–13]). Yet for closed membranes subject to both constraints of constant area and volume the problem is more complex, and the theoretical results obtained so far allow us at most to conclude that the k_c values deduced from fluctuation experiments are effective values, i.e., that they are different from the true bending modulus of a given type of membrane. An important point illuminated by the present study is that k_c measurements employing vesicle shape fluctuations can only be based on the *variances* of amplitudes of basis functions, because only the average shape can be determined from observations of the vesicle contours, whereas no direct information about the equilibrium shape is available. In order to deduce the value of k_c from the measured variances, one has to compare these variances with the corresponding theoretical predictions. However, since the predicted variances depend on the location of the vesicle in the phase diagram of equilibrium shapes, such predictions can only be made if the relative volume of the vesicle is known. In view of the results of Table I, this leads to a first uncertainty concerning the deduced k_c values. But even if the true relative volume could be estimated to a satisfactory degree of accuracy, one would still face the additional problem of a correct determination of the characteristic vesicle size R_S that enters the variances quadratically. If this characteristic size is estimated from the analysis of vesicle contours, the measurements will rather give the apparent vesicle size $\hat{R}_S$. Thus the measured *effective* bending modulus $\hat{k}_c$ would be related to the true modulus by

$$\hat{k}_c = k_c \left(\frac{\hat{R}_S}{R_S} \right)^2 = k_c (1 + \langle \Delta a_p \rangle) = k_c + \frac{k_B T}{8\pi} (\mu^{(a)} \ln l_{\max} + \eta^{(a)}), \quad (21)$$

which would give a value significantly smaller than k_c. It is noteworthy that for $\mu^{(a)}_{\text{flat}} = -2$ [cf. Fig. 6(a) and the above discussion on the logarithmic area reduction; Eq. (17)], this particular decrement of the bending modulus is in agreement with the result obtained in [12]. However, application of Eq. (21) to the interpretation of experimental observations would still leave the difficult task to estimate the relative volume of the vesicle. Therefore, this equation merely illustrates that the correction of the bending modulus is rather sensitive to the way in which the measurements are performed and to the use of any additional information about the vesicle parameters. Thus the deduction of the true bending modulus from fluctuation experiments seems to be generally problematic. On the other hand, most of these problems could be eliminated by an independent measurement of the vesicle's area and volume, e.g., by pipette aspiration as suggested above [20]. Furthermore, the present formalism enables us to systematically explore the behavior of a fluctuating vesicle in dependence on its location in the phase diagram of equilibrium shapes, and so it may provide another way to establish appropriate procedures for the interpretation of experimental results.

On conclusion of this section, it seems appropriate to comment on a few limitations of the present approach. First of all, our central result, the logarithmic dependence of the thermal shift on the number of degrees of freedom, was deduced from the results of our numerical calculations. It is left to future studies to verify this interesting finding analytically. Yet, considering that analytical approaches often involve a number of simplifying assumptions, a numerical treatment seems well justified when one's task is to simulate an experimental situation as accurately as possible. It should be mentioned that we have also applied the present formalism to the commonly used second-order model (e.g., [3]) that employs a second-order Taylor expansion in terms of the deviations of the vesicle shape from a sphere and that is valid only for nearly spherical vesicles. Within this model, the logarithmic dependence of the thermal shift can easily be derived analytically and the resulting coefficients agree well with those obtained by the present approach for nearly spherical vesicles. The details of this calculation have not been included in this paper mainly for the reason that some basic assumptions of our formalism break down for nearly spherical vesicles with relative volumes v_0 close to 1. In short, the problems are that (i) the subspace of states allowed by the constraints contracts into one point as $v_0 \to 1$, i.e., it is inadequate to allow infinitely large limits of integration in the integrals entering the expectation values, and (ii) the energy of the accessible states becomes more and more degenerate, so that the restriction to harmonic terms in the energy expansion is not justified anymore. In this case the results of the present approach, while mathematically still correct, would have little physical meaning. For this reason, we have chosen $v_0 = 0.95$ as the upper limit of relative volumes considered in this paper. Larger relative volumes would also cause another

problem concerning the experimental observation itself. All of our above comments on experiments have implied that the mean shape of the observed vesicle can easily be identified, so that also the orientation of the rotational axis of the mean shape is defined to a good approximation. In this case, our calculations correspond to experiments in which the rotational axis of the mean shape lies (more or less) in the focal plane. This is the experimental situation reported in [1], with the vesicle resting on the chamber bottom. On the other hand, as the vesicles become more spherical, it is hard to identify the orientation of the mean shape because the latter itself tends towards a sphere [cf., e.g., Figs. 4(a) and 5(a)] and because the distinction between deformational fluctuations and rotational diffusion of the vesicle is increasingly difficult. This effect may actually become quite important already at $v_0=0.95$ where the apparent relative volume $\langle \hat{v}_p \rangle$ at $l_{\max}=10^5$ is practically 1 (not included in Table I). However, $l_{\max}=10^5$ corresponds to extremely large vesicles and should be regarded as an upper limit for possible $l_{\max}$ values. For vesicle sizes not too large and for relative volumes $v_0 \leqslant 0.95$, experiments that can be related to the predictions of the present analysis are feasible [21].

Finally, it should be mentioned that our derivations were based on the assumption that the deviations from equilibrium are small. The fact that at typical k_c values the thermal shift in the shape of a giant vesicle tends to be rather large may thus add uncertainty to quantitative theoretical predictions. This applies in particular to predictions based on an extrapolation such as the one to large $l_{\max}$ values employed above. Thus the values of different quantities calculated for large values of $l_{\max}$ should be considered with caution; naturally, they can at most serve as rough estimates illustrating the general behavior of the fluctuating vesicle shape.

V. CONCLUSION

The present paper establishes a formalism to study thermal shifts and their effect on the correlation functions of thermally excitable systems that are subject to constraints. This concept is applied to thermal shape fluctuations of lipid vesicles taking place at constant values of the membrane area and the vesicle volume. The numerical results demonstrate large deviations of the thermal average shapes from the well-established equilibrium shapes. The concept of thermal shift and average shape is linked to the logarithmic reduction of the effective membrane area that has been studied so far only for flat membranes. Dependences of both the reduction of the membrane area as well as the reduction of the vesicle volume on the relative volume are presented and implications for related experiments are discussed.

ACKNOWLEDGMENTS

We would like to thank U. Seifert and M. Wortis for fruitful discussions. This work was funded by The Ministry of Science and Technology of the Republic of Slovenia Grant No. J3-7033-381-96.

[1] H.-G. Döbereiner, E. Evans, U. Seifert, and M. Wortis, Phys. Rev. Lett. **75**, 3360 (1995).
[2] U. Seifert, Z. Phys. B **97**, 299 (1995); M. Jarić, U. Seifert, W. Wintz, and M. Wortis, Phys. Rev. E **52**, 6623 (1995).
[3] M. Schneider, J. Jenkins, and W. Webb, J. Phys. **45**, 1457 (1984); J. F. Faucon, M. D. Mitov, P. Méléard, I. Bivas, and P. Bothorel, J. Phys. (Paris) **50**, 2389 (1989); H. Duwe, J. Käs, and E. Sackmann, *ibid.* **51**, 945 (1990); M. D. Mitov, J. Faucon, P. Méléard, and P. Bothorel, Adv. Supramol. Chem. **2**, 93 (1992); G. Niggemann, M. Kummrow, and W. Helfrich, J. Phys. (France) II **5**, 413 (1995).
[4] H. J. Deuling and W. Helfrich, J. Phys. (Paris) **37**, 1335 (1976); V. Heinrich, M. Brumen, R. Heinrich, S. Svetina, and B. Žekš, J. Phys. (France) II **2**, 1081 (1992); W. Wintz, H.-G. Döbereiner, and U. Seifert, Europhys. Lett. **33**, 403 (1996).
[5] V. Heinrich, S. Svetina, and B. Žekš, Phys. Rev. E **48**, 3112 (1993).
[6] S. Svetina and B. Žekš, Eur. Biophys. J. **17**, 101 (1989).
[7] U. Seifert, K. Berndl, and R. Lipowsky, Phys. Rev. A **44**, 1182 (1991); L. Miao, U. Seifert, M. Wortis, and H.-G. Döbereiner, Phys. Rev. E **49**, 5389 (1994).
[8] M. Peterson, J. Math. Phys. **26**, 711 (1985); J. Appl. Phys. **57**, 1739 (1985); M. Peterson, H. Strey, and E. Sackmann, J. Phys. (France) II **2**, 1273 (1992).
[9] P. G. de Gennes and C. Taupin, J. Phys. Chem. **86**, 2294 (1982).
[10] W. Helfrich, Z. Naturforsch. Teil C **30**, 841 (1975); W. Helfrich and R.-M. Servuss, Nuovo Cimento **3**, 137 (1984).
[11] L. Peliti and S. Leibler, Phys. Rev. Lett. **54**, 1690 (1985).
[12] W. Helfrich, J. Phys. (Paris) **46**, 1263 (1985).
[13] F. David and S. Leibler, J. Phys. (France) II **1**, 959 (1991).
[14] E. Evans and W. Rawicz, Phys. Rev. Lett. **64**, 2094 (1990).
[15] Throughout the paper, we abbreviate by ''correlation function'' the amplitude-amplitude correlation function of the deviations of the amplitudes of basis functions (chosen to describe the vesicle shape) from their equilibrium values.
[16] W. Helfrich, Z. Naturforsch. Teil C **28**, 693 (1973).
[17] B. Božič, S. Svetina, B. Žekš, and R. E. Waugh, Biophys. J. **61**, 963 (1992).
[18] V. Heinrich and R. E. Waugh, Ann. Biomed. Eng. **24**, 595 (1996).
[19] E. Evans and D. Needham, J. Phys. Chem. **91**, 4219 (1987).
[20] We note that the determination of k_c is further complicated in view of two more control parameters involved through the nonlocal bending energy, i.e., the nonlocal bending modulus and the reference difference of monolayer areas. It is left to future studies to establish the range in the phase diagram of equilibrium shapes where nonlocal bending effects become important. The observations reported in [1] certainly belong to this range.
[21] V. Heinrich *et al.* (unpublished).